

# Numerical Simulation of a Transformer-Based Test Platform

P. Quintanilla<sup>\*1</sup>, E. Sainz<sup>1</sup>, R. Altay<sup>2</sup>, A. Santisteban<sup>1</sup>, F. Ortiz<sup>1</sup>, and A. Ortiz<sup>1</sup>

<sup>1</sup>*Department of Electrical Engineering, University of Cantabria, Spain*

<sup>2</sup>*R&D Department, BEST Transformer, Türkiye*

\*quintanillap@unican.es

**Abstract**—This paper investigates the utilization of esters in power transformers for their cooling and dielectric insulation properties, focusing on their potential to enhance safety and reduce environmental impact. A test platform based on a 100MVA power transformer was developed to analyze the performance of these alternative fluids in an ONAN operation regime. Using Finite Volume Method-based tools and Thermo-Hydraulic Network Models, calculations were conducted to compare the fluid behavior of an ester and a mineral oil within the test platform. The results present thermal and hydraulic data for both types of fluids, highlighting their compatibility with the transformer and adherence to industry standards. The study concludes by demonstrating the feasibility of esters for sustainable power systems and the utility of numerical simulations in predicting fluid dynamics, affirming the effectiveness of the experimental setup.

**Keywords**—Dielectric, Ester, Numerical Simulation, ONAN, Power Transformer, Test Platform, Thermo-Hydraulic Model.

## I. INTRODUCTION

In electrical systems, power transformers play a crucial role in enabling the efficient transmission of electricity over long distances. Given their cost and importance for system stability, reliability, and safety, ensuring their longevity, and maintaining optimal conditions for both the transformer and the power grid is imperative, as demonstrated by Cepeda et al. in 2014 [1]. Therefore, the primary consideration for their upkeep is the insulation components and their susceptibility to overloads, upon which they depend.

Examining the impact of load on transformer thermal distribution and its implications for safety holds significance in the realm of cooling systems. This inquiry not only mitigates the risk of overheating and failures but also contributes machine longevity through management of the degradation of dielectric materials. The employment of numerical models to conduct such investigations is widespread. These models are usually of two complementary types: 1) Modeling tools made ad hoc for the geometry and the specific scenario. This typology is usually known as thermohydraulic network models (THNM) and consists of two models coupled together that allow the average distribution of temperatures and velocities in the domain to be determined iteratively. 2) Commercial or Open-source tools based on the Finite Volume Method (FVM) and that allow the transient or stationary behavior of the model to be calculated with great precision. Regarding the first of these tools, in 2010, Radakovic et al. showed in [2], the application of THNM to power transformer specifying the type of winding also considering the effect of the closed circuit that occurs in the transformer through the passage of the fluid through windings, tank, ducts and radiators. In 2017, Rios et al. published a wide study about fluid behavior in the radiator of

a power transformer through thermal modelling [3]. On the other hand, there are numerous studies that cover fluid dynamic behavior with FVM. In 2019, Santisteban et al. presented in [4], a comparison between the results with the two mentioned methodologies applied to a transformer immersed in oil, in turn carrying out the analysis to several alternative dielectric fluids in the disc-type winding. Altay et al. presented in the same period, the fluid-dynamic behavior of the layer winding of a 100MVA power transformer considering different alternative dielectric fluids [5].

The importance of analyzing alternative fluids, as discussed in [4] and [5], is well established. Transitioning to alternative dielectric fluids, such as natural or synthetic esters, is crucial due to environmental protection and fire risk reduction. Mineral oil (MO) poses environmental risks such as soil and water contamination, while its production and disposal contribute to greenhouse gas emissions. Additionally, its low flash and fire points increase the risk of fires, posing threats to human safety and the environment. Adopting alternatives like natural esters from renewable sources or synthetic esters provides a dual benefit: reduced environmental impact and enhanced safety. This was highlighted by Haegele et al. in 2018 [6] and Mendez et al. in 2023 [7]. These fluids have higher biodegradability, lower toxicity, and increased fire resistance, aligning with sustainability objectives while mitigating potential disasters.

In addition to the computational techniques mentioned earlier for analyzing the thermal and hydraulic behavior of transformers, experimental platforms have been developed in recent years. These platforms aim to replicate certain transformer zones in the real world for analysis, improvement, or validation of models in a more cost-effective and straightforward manner. In this regard, the work of Torriano et al. [8], published in 2018, is noteworthy. It exhibits the application of Computational Fluid Dynamics (CFD) to a platform designed for the investigation of a transformer.

The present study focuses on the development and analysis of an experimental platform replicating the exposed power transformer in [5], utilizing THNM and CFD simulations to predict the behavior of a transformer changing its oil to an ester. Through this platform, a range of experimental scenarios can be investigated, providing valuable insights into transformer performance in real-world conditions. This research contributes to the ongoing efforts to optimize transformer design and operation, aiming to create more sustainable and efficient power systems taking into account at all studies the technical limits set by IEC and IEEE standards [9]-[10]. In this way, an ester is applied to compare alternative fluid behaviors to traditional mineral oil ones.

## II. DESCRIPTIONS OF THE MODELS

Before outlining the analysis methodologies used to predict the temperature and velocity fields of the test platform, it is necessary to define the geometric design that has been considered as the reference. In broad terms, the most notable elements are: 1) The heating zone that is inside of the tank, which has two plates of kraft insulation. Between these two insulating plates, there are five additional layers formed by Continuously Transposed Conductor (CTC) through which the 9200W of electrical losses from the transformer's Low-Voltage Winding (LVW) are transferred to the dielectric fluid encasing them; and 2) The cooling zone, composed of radiator fins directly sized from the original electrical machine.

The experimental platform has been configured to align with the real transformer's specifications. Parameters such as winding height, distance of radiator and winding centers, layer thickness, radiator height, and radiator depth were directly transposed from the real transformer. Furthermore, key elements crucial for the design, including layer thermal conductivity, layer heat capacity, radiator fin number, heat losses for LVW, and tank oil capacity, have been calculated throughout the manufacturing or ad hoc design process. This comprehensive approach ensures that the experimental setup faithfully represents the real transformer, facilitating precise analysis and comparison of performance metrics.

The CTC layers have dimensions of 1634(H) x 1200(L) x 16(W) mm, with a separation of 6mm between them as well as between the outermost layers and the vertical insulation plates. The insulation plates width is 3mm while the heater layer one is 16mm. The height from the center of the radiators to the center of these heaters is 0.565m. This radiator is composed of thirteen fins. Each fin has a height of 2.1m, a thickness of 6mm, and a maximum width of 0.45m. The ducts connecting the tank to the radiator have a diameter of 80mm. Figure 1 illustrates the platform configuration, separating ducts to detail main components, omitting tube length and measurement elements. Thermal losses in them were neglected for calculations.

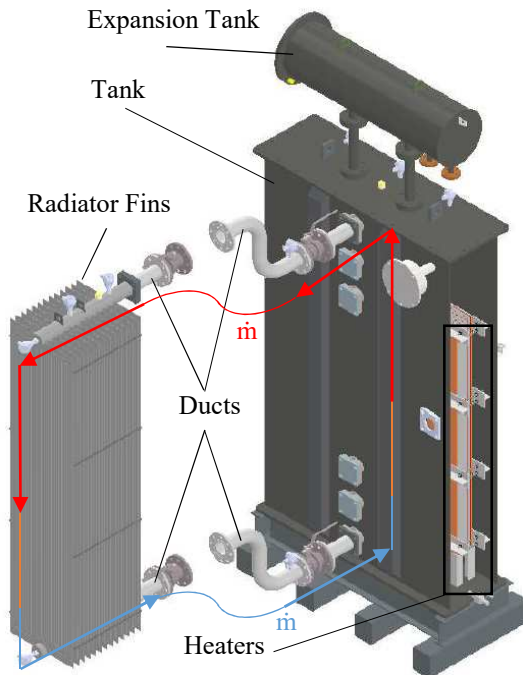


Figure 1. Experimental Platform Scheme

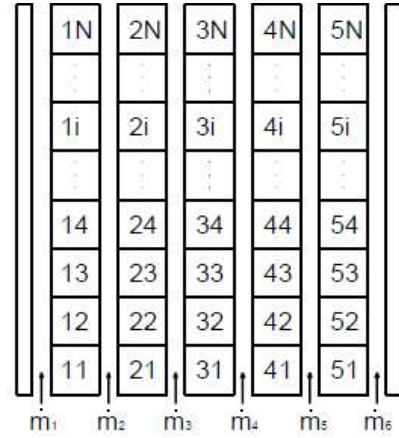


Figure 2. Layer-type Winding Scheme

Figure 2 illustrates the scheme considered in the winding (LVW layers of the heater) and the two-dimensional flow inlet within the winding.

To compare the outcomes of the CFD and THNM approaches, identical boundary conditions are implemented in each model:

- All exterior solid walls of the geometric model are considered adiabatic.
- At all the walls of the cooling channels, the no-slip condition is applied.
- It is assumed that the heat loss distribution is constant and uniform throughout the entire winding.
- The inlet temperature and mass flow are constant while the outlet pressure is zero.

The heat transfer coefficient applied in cooling zone has been based on information provided by the commercial simulation software for the materials used in the radiator to transfer heat to the surroundings, which is approximately 8 W/m<sup>2</sup>K for the working temperature range.

### A. CFD Model

Before proceeding with the spatial discretization of the geometry and the calculation of the system applying the governing equations, two complementary models have been developed: 1) A total planar 2D geometry forming a closed loop, and 2) A three-dimensional geometry representing the layer-type winding zone. These models have been used to cross-validate each other's fidelity to reality and the adequacy of the solving method and boundary conditions in the partial 3D model. The details of 2D model were exposed by Quintanilla et al. in 2022 [11].

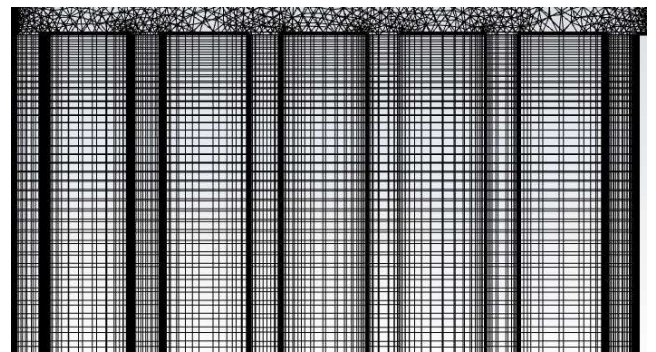


Figure 3. 3D Detailed winding Mesh in a x-axis projection

### 1) Spatial Discretization

The 3D model has a mesh of 1,221,716 elements. A minimum division of 10 cells has been maintained in each channel to achieve a considerable level of accuracy. Hexahedral cells have been created in the majority of the domain, as shown in Fig. 3, which is the projection in the x-axis of the heating zone mesh.

### 2) Material Assignments

To simplify the model, thermal properties of Table I have been used, where the layers representing the LVW are composed of properties of CTC, while the vertical insulation plates have been kept as spaces outside the domain. The fluids have also been applied separately to the models, initially using mineral oil for validation, and subsequently applying the properties of ester to observe the difference in behavior and the potential viability of the dielectric fluid.

TABLE I. THERMAL PROPERTIES

|                               | Mineral oil   | Ester   | CTC                        |
|-------------------------------|---|---|----------------------------|
| Density (kg/m <sup>3</sup> )  | 1053.3-0.655T   | 1157-0.65T  | 8979                       |
| Thermal Conductivity (J/kg-K) | 0.1509 - 7.101·10 <sup>-5</sup> T   | 0.0971 + 3.74·10 <sup>-4</sup> T - 7.25·10 <sup>-7</sup> T <sup>2</sup> | 0.68 X axis<br>1.32 Y axis |
| Heat Capacity (W/m-K)         | 807 + 3.58T   | 1242 + 2.198T   | 381                        |
| Viscosity (kg/m-s)            | 0.34024 - 2.402·10 <sup>-3</sup> T +5.671·10 <sup>-6</sup> T <sup>2</sup> | 2.398254 - 0.0181T +4.567·10 <sup>-5</sup> T <sup>2</sup>               | -                          |

### 3) Governing Equations

This model is based on the solving of partial differential equations that govern the flow. Due to the type of flow that it is expected in the fluid circuit, it has been treated as laminar and incompressible. Equations (1)-(3) express the conservation of mass, momentum, and energy in the fluid domain while (4) represents the conservation of energy in the solid domain.

$$\frac{\partial \rho}{\partial t} + \nabla(\rho \vec{v}) = 0 \quad (1)$$

$$\frac{\partial(\rho \vec{v})}{\partial t} + \nabla \cdot (\rho \vec{v} \vec{v}) = -\nabla p + \mu(\nabla^2 \vec{v}) + \vec{g}(\rho - \rho_{ref}) \quad (2)$$

$$\frac{\partial(\rho C_p T)}{\partial t} + \nabla(\rho C_p \vec{v} T) = \nabla \cdot (k \nabla T) + S_h \quad (3)$$

$$\frac{\partial}{\partial t}(\rho C_p T) = \nabla \cdot (k \nabla T) + S_h \quad (4)$$

Being  $\rho$ ,  $\vec{v}$ ,  $\mu$ ,  $g$ ,  $C_p$ ,  $T$ ,  $k$ , and  $S_h$  density, velocity vector, dynamic viscosity, gravity, specific heat capacity, temperature, thermal conductivity, and volumetric heat source, respectively.

#### B. Thermo-Hydraulic Network Model

THNM is a method relying on conservation laws of mass, momentum, and energy. It involves two interconnected networks (hydraulic and thermal) used to model systems like cooling or heating channels. The solid domain is solved akin to CFD, while the fluid domain is addressed using one-dimensional coefficients such frictional pressure drops, local

pressure drops and Nusselt coefficients, impacting model accuracy.

Deviations between the hydraulic and thermal models are due to differing fluid domain solutions. THNM assumes fully developed flow and perfect thermal/hydraulic mixing, with frictional pressure drop treated separately via a friction coefficient, analytically expressed for isothermal laminar flow. These distinctions necessitate separate expressions for frictional and local pressure drops in the fluid domain, contributing to deviations between models.

For local pressure drops, coefficients have been calculated using correlations obtained from experimental data, as presented in [12]. Moreover, it has been also utilized to compute the Nusselt coefficients.

Initially, implementing the THNM on the platform's geometry, a working point is obtained where the mass flow rate circulating through the heating zone is obtained supposing same power losses. This calculated point, derived from the intersection of the driving pressure equation (5) and the pressure drops equation (6) together with frictional pressure drop in the circuit, initiates the model calculation considering the approximations mentioned in section II.A.

$$p_t = \rho_r \cdot g \cdot \Delta T_{oil} \cdot \Delta H \quad (5)$$

$$\Delta p = \xi \frac{\rho \cdot v^2}{2} \quad (6)$$

Being  $\Delta T_{oil}$ ,  $\Delta H$ ,  $\xi$  the temperature vertical gradient, height difference between geometrical centers of layers and the radiator and the pressure drop coefficient, respectively.

All numerical model simulations have been run with ANSYS Fluent 2023-R1 on a Dell Precision 7960 Tower computer that has 256 GB of RAM and an Intel Xeon w9-3495X processor (56 processors at 1.896 MHz).

## III. RESULTS AND VALIDATION

In this section, the results obtained from the analysis are presented, including the values that have been experimentally measured for validation.

Due to the nature of the study, the focus is on the thermal distribution, given the simple hydraulic circuit consisting solely of vertical fluid channels. In [11], it was discussed the platform's adaptation to the real transformer; however, for the current validation, results from the actual platform are available and considered accurate for validating the model in this study. Figures 4a and 4b depict the thermal distribution results from the 3D CFD simulation in the upper part of the channels using mineral oil or an ester respectively. Additionally, for comparative purposes, thermal distributions in the layers are shown in Fig. 4c, based on the type of refrigerant used, whether mineral oil or ester. This is further illustrated with the color map shown in Fig. 4d.

In addition to the CFD analysis results, it is crucial to verify the thermo-hydraulic modeling with both fluids. The most representative thermal data from this analysis can be seen in Table II. With this information, the validation can be accepted as accurate. The experimental values were obtained from thermal images, as shown in [11], and from Fiber Optic Sensors (FOS) placed at heights of the winding close to the predicted Hot-Spot Temperature (HST) location.

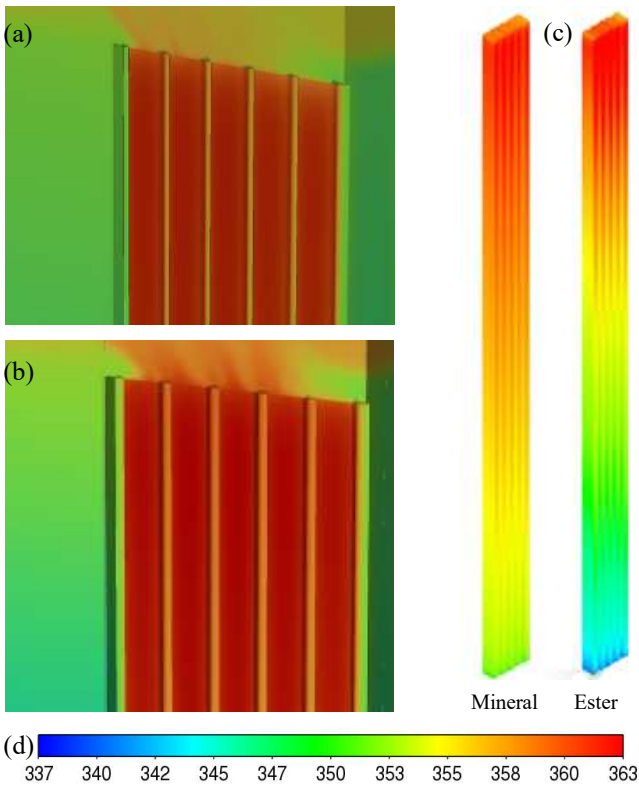


Figure 4. Layer Winding Temperature distribution in 3D CFD Simulation. Results in channels with Mineral Oil (a) and Ester (b). Temperature distribution in solid layers (c) and the colormap in Kelvin (d)

Furthermore, RTD PT100 sensors have been allocated at different points of the flow path. In this way, it has been possible to validate from the top oil, radiator, and bottom tank points. Although validation can be accepted for both numerical simulation methodologies, it should be noted that while the execution time of THNM has been a few seconds, the CFD model requires calculation time of many hours for the mentioned hardware. However, the higher accuracy of the results of the CFD model is observed.

Upon verifying the values obtained with both tools, we observe not only their agreement but also adherence to the limits of the IEC 60076-14 [9] and IEEE STD C57.154 [10] standards. It is worth noting that the thermal values using ester obtained in the 3D simulation (the only simulation where comparison is possible) would provide a greater safety margin from a thermal perspective (maximum 130°C in top oil and 140°C in HST) compared to mineral oil (105°C in top oil and 120°C in HST).

TABLE II. TEMPERATURE RESULTS AND VALIDATION

|                           | Experiment (MO)                   | CFD (MO)  | CFD Ester | THNM (MO) | THNM Ester |
|---------------------------|-----------------------------------|-----------|-----------|-----------|------------|
| HST                       | 89 °C (FOS)                       | 88 °C     | 89 °C     | 91 °C     | 94         |
| Top Oil Temperature       | 80 °C (PT100)                     | 79 °C     | 81 °C     | -         | -          |
| Average layer Temperature | 83 °C (FOS at top part of layers) | 73 °C     | 73 °C     | 80 °C     | 81 °C      |
| Average mass-flow         | 0.9 kg/s <sup>a</sup>             | 0.83 kg/s | 0.56 kg/s | 0.73 kg/s | 0.5 kg/s   |

<sup>a</sup>Measured in the main duct. Winding mass-flow should be close to 95% of the shown value.

#### IV. CONCLUSIONS

A numerical simulation analysis of two fluids – mineral oil and ester – has been presented for use in an experimental platform. This machine, designed to validate new methodologies quickly, affordably, and easily analyzed, shows its correct validation both in the previous calculations and the measured experimental solution, as well as in two numerical simulation methodologies. Although the accuracy of the results has been higher in the CFD models, the calculation time has been much higher in THNM. Additionally, the results presented suggest a promising thermal performance from an alternative fluid in the original power transformer. Hence, this study is considered a step towards demonstrating the good thermal performance that these liquids can provide, paving the way for their application. This application will be beneficial due to their qualities regarding environmental damage and fire risk mitigation.

#### ACKNOWLEDGMENT

The authors are grateful to the Spanish Ministry of Science and the European Commission for their support through the approval of projects PID2019-107126RB-C22 and MSCA2018-RISE-823969, respectively.

#### REFERENCES

- [1] J. Cepeda y D. G. . Colomé, «Evaluación de la Vulnerabilidad del Sistema Eléctrico de Potencia en Tiempo Real usando Tecnología de Medición Sincrofásorial», re, vol. 10, n.º 1, pp. PP. 91–101, ene. 2014
- [2] Z. R. Radakovic and M. S. Sorgic, "Basics of detailed thermo-hydraulic model for thermal design of oil power transformers," IEEE Transactions on Power Delivery, vol. 25, no. 2, pp. 790-802, 2010.
- [3] G. R. Rodríguez, L. Garelli, M. Storti, D. Granata, M. Amadei, and M. Rossetti, "Numerical and experimental thermo-fluid dynamic analysis of a power transformer working in ONAN mode," Applied Thermal Engineering, vol. 112, pp. 1271-1280, 2017.
- [4] R. Altay Et Al., "Use Of Alternative Fluids In Very High-Power Transformers: Experimental And Numerical Thermal Studies," In Ieee Access, Vol. 8, Pp. 207054-207062, 2020, Doi: 10.1109/Access.2020.3037672.
- [5] A. Santisteban, A. Piquero, F. Ortiz, F. Delgado, and A. Ortiz, "Thermal modelling of a power transformer disc type winding immersed in mineral and ester-based oils using network models and CFD," IEEE Access, vol. 7, pp. 174651-174661, 2019.
- [6] S. Haegele, F. Vahidi, S. Tenbohlen, K. J. Rapp, y A. Sbravati, "Lightning impulse withstand of natural ester liquid," Energies, vol. 11, no. 8, pp. 1964, 2018.
- [7] C. M. Gutiérrez, A. O. Fernández, C. J. R. Estébanez, C. O. Salas, y R. Maina, "Understanding the ageing performance of alternative dielectric fluids," IEEE Access, vol. 11, pp. 9656-9671, 2023.
- [8] F. Torriano, H. Campelo, M. Quintela, P. Labbé, and P. Picher, "Numerical and experimental thermofluid investigation of different disc-type power transformer winding arrangements," International Journal of Heat and Fluid Flow, vol. 69, pp. 62-72, 2018.
- [9] IEC 60076, "Power Transformers," International Electrotechnical Commission, 2014.
- [10] IEEE STD C57.154, "IEEE Standard For The In-Service Monitoring Of Mineral-Insulating Oil In Electrical Equipment," Ieee, 2012.
- [11] P. Quintanilla, R. Altay, A. Santisteban, A. Ortiz, y K. Koseoglu, "CFD analyses of a test platform with different fluids for use in transformers," in 2022 7th International Advanced Research Workshop on Transformers (ARWtr), pp. 48-51, IEEE, October 2022.
- [12] I. E. Idelchik, Handbook of Hydraulic Resistances. Boca Raton, FL: CRC, 199.